

Role of Many-Body Effects in Describing Low-Lying Excited States of π -Conjugated Chromophores: High-Level Equation-of-Motion Coupled-Cluster Studies of Fused Porphyrin Systems

K. Kowalski*

William R. Wiley Environmental Molecular Sciences Laboratory, Battelle, Pacific Northwest National Laboratory, K8-91, P.O. Box 999, Richland, Washington 99352, United States

R. M. Olson

Cray, Incorporated, 380 Jackson St. Suite 210, St. Paul, Minnesota 55101, United States

S. Krishnamoorthy

High Performance Computing, Pacific Northwest National Laboratory, Richland, Washington 99352, United States

V. Tippuraju and E. Aprà*

Computer Science and Mathematics Division, Oak Ridge National Laboratory, Oak Ridge, Tennessee 37831, United States

ABSTRACT: The unusual photophysical properties of the π -conjugated chromophores make them potential building blocks of various molecular devices. In particular, significant narrowing of the HOMO–LUMO gaps can be observed as an effect of functionalization chromophores with polycyclic aromatic hydrocarbons (PAHs). In this paper we present equation-of-motion coupled cluster (EOMCC) calculations for vertical excitation energies of several functionalized forms of porphyrins. The results for free-base porphyrin (FBP) clearly demonstrate significant differences between functionalization of FBP with one- (anthracene) and two-dimensional (coronene) structures. We also compare the EOMCC results with the experimentally available results for anthracene fused zinc–porphyrin. The impact of various types of correlation effects is illustrated on several benchmark models, where the comparison with the experiment is possible. In particular, we demonstrate that for all excited states considered in this paper, all of them being dominated by single excitations, the inclusion of triply excited configurations is crucial for attaining qualitative agreement with experiment. We also demonstrate the parallel performance of the most computationally intensive part of the completely renormalized EOMCCSD(T) approach (CR-EOMCCSD(T)) across 120 000 cores.

INTRODUCTION

The remarkable photophysical properties of the π -conjugated chromophores, emanating from very small HOMO–LUMO gaps, has recently stimulated a lot of interest. Of special interest are the π -conjugated porphyrin arrays, where the existence of low-lying excited states in the near-infrared absorption spectra makes these systems potential building blocks for molecular wires, optical devices, and light-harvesting systems (for a review of this broad area, see refs 1–10 and references therein). Over the last 2 decades it has been experimentally demonstrated that tuning the electronic structure of these systems is especially efficient when porphyrins are functionalized with the polycyclic aromatic hydrocarbons (PAHs). Theoretical studies of excited states can be very helpful in understanding the impact of various types of functionalization and can predict shifts in absorption spectra. For this purpose, various ab initio methodologies can be used. In addition to providing accurate and predictive results that can be compared with experiment, these wave-function-based ab initio approaches are also important to calibrate and parametrize low-order Hamiltonians.^{11–16} On the other hand, due to the size of

these systems and steep scaling of the high-level excited-state methods, examples of high-level calculations for these molecules are very scarce. For example, the current literature does not show any systematic study of the role played by higher-order effects (for example, collective three-body excitations) for functionalized forms of the porphyrins.

Another important question concerns possible ways of incorporating important excited-state correlation methods. Among many methods, the equation-of-motion of coupled cluster method (EOMCC)^{17–20} (for related approaches see refs 21–30) has evolved into a widely used formalism for calculating vertical excitation energies (VEEs). The well-established family of approximations including higher excitations starting from the rudimentary EOMCCSD model (EOMCC with singles and doubles)^{18–20} to more expensive models with triples (EOMCCSDT)³¹ and quadruples (EOMCCSDTQ),³² etc., have enabled one to reach the full configuration interaction (FCI) limit when all possible

Received: March 30, 2011

Published: May 27, 2011

excitations are included. The EOMCCSD can be used to describe singly excited states, whereas more complex excited states require the expensive EOMCCSDT approximation. In order to find a trade-off between cost and accuracy, in this paper we will resort to the completely renormalized EOMCCSD(T) approach (CR-EOMCCSD(T)),³³ which accounts for the effect of triply excited configurations in a noniterative manner (see also ref 34) and at the same time is characterized by the N^7 scaling (N represents the system size). For systems of the size of the functionalized porphyrins, the applicability of high-order methods faces significant challenges, mostly associated with the very steep numerical scaling. Therefore, in order to make these methods applicable to π -conjugated chromophores, their efficient parallel implementations need to be used.

In this paper, we want to address the following problems: (1) What is the role of various-rank correlation effects in describing the vertical excitation energies in fused porphyrins, and what level of approximation and basis set are required to obtain an agreement of calculated VEEs with the experimentally inferred values? In particular, we will analyze the effect of including triply excited amplitudes. We will illustrate the accuracies of the EOMCCSD and CR-EOMCCSD(T) methods on the example of available experimental data for the anthracene fused zinc-porphyrin.⁷ (2) What is the effect of functionalizing free-base porphyrin by adding one- and two-dimensional structures, anthracene and coronene? (3) How can efficient computer implementations exploit massively parallel computer architectures?

THEORY

The EOMCC formalism has evolved into one of the most widely used tools in excited-state calculations of low-lying excited states,¹⁷ where various correlation effects can be controlled by the rank of excitations included in the cluster (T) and correlation (R_K) operators used to parametrize K th excited state

$$|\Psi_K\rangle = R_K e^T |\Phi\rangle \quad (1)$$

where $|\Phi\rangle$ is the so-called reference function usually chosen as a Hartree–Fock determinant. Various approximation schemes range from the basic EOMCCSD approximation, where the cluster and correlation operators are represented as sums of scalar ($R_{K,0}$ for excitation operator only), single ($T_1, R_{K,1}$), and double ($T_2, R_{K,2}$) excitations,

$$|\Psi_K^{\text{EOMCCSD}}\rangle = (R_{K,0} + R_{K,1} + R_{K,2}) e^{T_1 + T_2} |\Phi\rangle \quad (2)$$

to the more accurate EOMCCSDT approach. Over the last 2 decades it was demonstrated that the progression of methods: EOMCCSD → EOMCCSDT → EOMCCSDTQ... leads to more accurate estimates of the excited-state energies, which in the limit of N_e (N_e stands for the number of correlated electrons) excitations converge to the FCI energies. However, the rapid growth in the numerical complexity [N^6 (EOMCCSD), N^8 (EOMCCSDT), N^{10} (EOMCCSDTQ)] of the EOMCC methods makes accurate calculations with the EOMCCSDT and EOMCCSDTQ methods prohibitively expensive, even for relatively small systems. Unfortunately, the EOMCCSD method is capable of providing reliable results only for singly excited states. However, as it has recently been demonstrated,³⁵ conspicuous errors in the range of 0.25–0.30 eV with respect to the experimental VEEs persist with increasing system size. In order to narrow the gap between the EOMCCSD and EOMCCSDT VEEs, several noniterative N^7 -scaling methods that mimic the

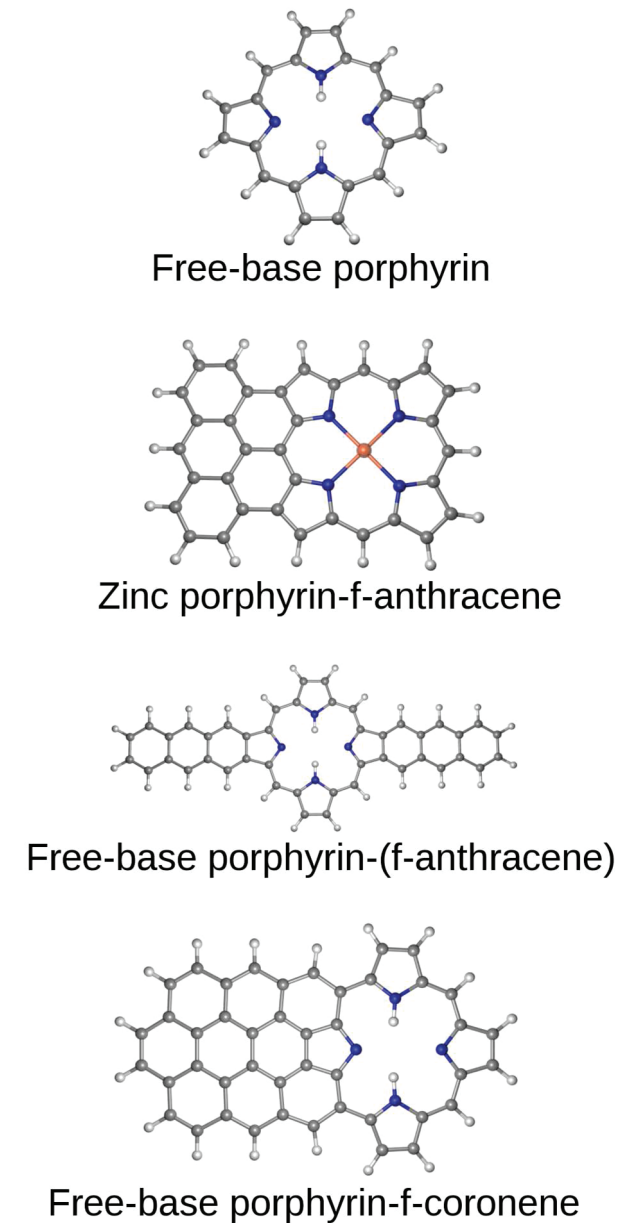


Figure 1. Benchmark set of molecules considered in this study.

effect of triples in a perturbative fashion have been proposed in the past.^{36–41} The completely renormalized EOMCCSD(T) approach (CR-EOMCCSD(T))³³ falls into this category (see also refs 42 and 43 for the most recent developments). In this approach, the energy correction $\delta_K^{\text{CR-EOMCCSD}(T)}$ is added to the EOMCCSD VEE ($\omega_K^{\text{EOMCCSD}}$)

$$\omega_K^{\text{CR-EOMCCSD}(T)} = \omega_K^{\text{EOMCCSD}} + \delta_K^{\text{CR-EOMCCSD}(T)} \quad (3)$$

where the $\delta_K^{\text{CR-EOMCCSD}(T)}$ is expressed through the trial wave function $\langle \Psi_K |$ and the triply excited EOMCCSD moment operator $M_{K,3}^{\text{EOMCCSD}}$ (see ref 33 for details)

$$\delta_K^{\text{CR-EOMCCSD}(T)} = \frac{\langle \Psi_K | M_{K,3}^{\text{EOMCCSD}} | \Phi \rangle}{\langle \Psi_K | (R_{K,0} + R_{K,1} + R_{K,2}) e^{T_1 + T_2} | \Phi \rangle} \quad (4)$$

The N^7 scaling of the CR-EOMCCSD(T) method stems from the $M_{K,3}^{\text{EOMCCSD}}|\Phi\rangle$ part. Although the CR-EOMCCSD(T) method has the same N^7 scaling as the ground-state CCSD(T) method,⁴⁴ there is a numerical prefactor that makes our CR-EOMCCSD(T) implementation 3 times more expensive for the states of the same symmetry as the ground state and 2 times more expensive for states of different symmetry than the ground state. Moreover three (two) large two-body intermediates of the size proportional to the $n_o n_u^3$ (n_o and n_u refer to the number of occupied and unoccupied spin-orbitals) have to be formed in the calculation of excited states of the same (different) symmetry as the ground state. Therefore, the storage of these quantities requires substantial memory resources. These requirements can be significantly reduced in the active-space CR-EOMCCSD(T) methods.³⁵

Table 1. A Comparison of the EOMCCSD and CR-EOMCCSD(T) VEEs (in eV) for the Two Lowest Singlet States of the Anthracene Molecule in Various Basis Sets

basis set	EOMCCSD	CR-EOMCCSD(T)
	$^1\text{L}_a$ State, Expt 3.60 eV ⁶²	
AVTZ	4.48	4.22
cc-pVDZ	4.16	3.87
POL1	4.00	3.69
	$^1\text{L}_b$ State, Expt 3.64 eV ⁶²	
AVTZ	4.00	3.76
cc-pVDZ	3.96	3.68
POL1	3.90	3.59

Table 2. EOMCCSD and CR-EOMCCSD(T) VEEs (in eV) for the Coronene Molecule in Various Basis Sets

basis set	EOMCCSD	CR-EOMCCSD(T)
	$^1\text{L}_b$ State	
AVTZ	3.46	3.22
cc-pVDZ	3.43	3.16
POL1	3.38	3.10
cc-pVTZ	3.40	3.08
	$^1\text{L}_a$ State, Expt 3.72 eV ⁶⁸	
AVTZ	4.48	4.25
cc-pVDZ	4.17	3.92
POL1	4.08	3.81
cc-pVTZ	4.07	3.77

COMPUTATIONAL DETAILS

All calculations were performed with a development version of NWChem suite of codes.⁴⁵ The EOMCC calculations were carried out with the TCE⁴⁶ implementations of the EOMCCSD and CR-EOMCCSD(T) methods. In all calculations we used the development variant of the CR-EOMCCSD(T) code, which significantly reduces the local memory requirements. In particular, the new implementation offers the possibility of partitioning six-dimensional tensors across the first two dimensions, which enables one to use large-size tiles (or basic building block defining the partitioning of spin-orbital domain and block structure of all tensors), which significantly improves the performance of the iterative part (CCSD and EOMCCSD). Iterative CCSD and EOMCCSD have also undergone significant changes. A major problem in the older implementation was “serial” execution of parallel procedures characterized by task pools of various size. This “vertical” structure has been replaced by a horizontal structure where all procedures are grouped into several classes, each class containing procedures that can be executed independently of each other. All subroutines from a given class contribute to a global task pool characterizing given class, which to a large extent alleviates the problems associated with load balancing. All tensors corresponding to cluster/excitation amplitudes, recursive intermediates, and electron integrals were stored on global arrays, which provide a portable shared-memory interface.

In our calculations, we considered several systems (some of them shown in Figure 1): (1) anthracene, (2) coronene, (3) free-base-porphyrin (FBP), (4) fused anthracene–Zn–porphyrin (ZnP-f-anthracene), (5) double anthracene fused free-base porphyrin [FBP-(f-anthracene)₂] (oligoporphyrin **46** of ref 10), and (6) coronene fused free-base porphyrin (FBP-f-coronene) (oligoporphyrin **65** of ref 10). Except for the anthracene and FBP, geometries of the remaining systems were optimized with the B3LYP approach⁴⁷ using the cc-pVTZ basis set.^{48,49} The geometries of anthracene and FBP are the same as used in refs 50 and 51, respectively. In all correlated calculations the core electrons were kept frozen. The calculations for anthracene were performed using Ahlrichs’ VTZ (AVTZ),⁵³ cc-pVDZ, and POL1⁵² basis sets. For coronene, AVTZ, cc-pVDZ, POL1, and cc-pVTZ basis sets were employed. For larger systems, we used AVTZ (FBP, ZnP-f-anthracene, FBP-f-coronene) and cc-pVDZ (FBP, ZnP-f-anthracene, FBP-(f-anthracene)₂) basis sets. Our calculations were performed with D_{2h} [anthracene, coronene, FBP, FBP-(f-anthracene)₂] and C_{2v} (ZnP-f-anthracene, FBP-f-coronene) symmetries. For larger systems we used relaxed convergence criteria for iterative approaches. Previous studies with the

Zinc porphyrin-f-anthracene

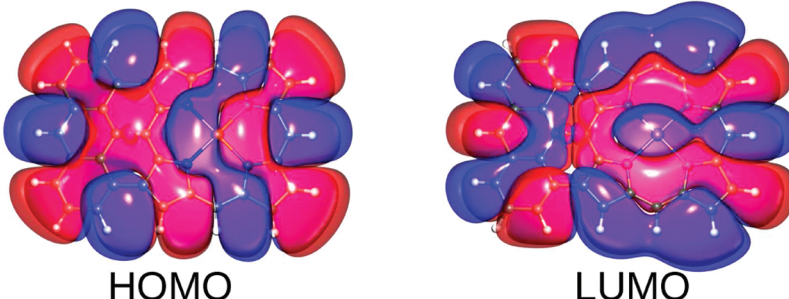


Figure 2. Graphical representation of the RHF HOMO and LUMO orbitals for the ZnP-f-anthracene system obtained with the cc-pVDZ basis set.

EOMCC methods³⁵ suggest that the cc-pVDZ basis set can provide reliable results for valence excited states for systems as large as an oligoporphyrin dimer. The issue of basis set choice will be discussed in the next section.

■ DISCUSSION

The ZnP and FBP systems have been studied intensively by employing the EOMCCSD, CR-EOMCCSD(T), and active-space CR-EOMCCSD(T) methods. In studies of the effect of the functionalization of the porphyrins, we will refer to the results available in the literature.^{35,54} We start our discussion by presenting the VEEs of the two lowest-lying singlet–singlet $\pi \rightarrow \pi^*$ transitions for components of our target systems: anthracene and coronene. We will employ the Platt nomenclature⁵⁵ for these

Table 3. EOMCCSD and CR-EOMCCSD(T) VEEs (in eV) for the ZnP-f-anthracene System in AVTZ and cc-pVDZ Basis Sets

basis set	EOMCCSD	CR-EOMCCSD(T)
¹ L _a State, Expt. 1.71 eV ⁷		
AVTZ	2.03	1.79
cc-pVDZ	2.03	1.77
dominant excitation ^a	H→L	

^a See the text for details.

Table 4. A Comparison of the EOMCC VEEs (in eV) of the FBP-(f-anthracene)₂ and FBP-f-coronene with the VEEs (in eV) of the Free-Base Porphyrin Using cc-pVDZ and AVTZ Basis Sets, Respectively

FBP-(f-anthracene) ₂ (cc-pVDZ)		FBP(cc-pVDZ) ^a	
		¹ B _{3u}	¹ B _{2u}
EOMCCSD	1.99	2.57	2.15
CR-EOMCCSD(T)	1.78	2.37	1.86
dominant excitation ^b	H→L	H-1→L	H-1→L H→L
		H→L+1	H→L+1 H-1→L+1
FBP-f-coronene (AVTZ)		FBP(AVTZ)	
		¹ B _{3u}	¹ B _{2u}
EOMCCSD	1.63	—	2.15
CR-EOMCCSD(T)	1.36	—	1.88
dominant excit. ^b	H→L	H-1→L	H→L
		H→L+1	H-1→L+1

^a From ref 35. ^b See the text for details.

excited states, ¹L_a and ¹L_b, where these states are dominated by HOMO→LUMO excitation (L_a) and a combination of HOMO→1→LUMO and HOMO→LUMO+1. Since the excited states of porphyrin-anthracene and porphyrin-coronene complexes studied in this paper have similar configurational structure we will adapt the Platt convention to characterize these states. Using NWChem (autosym) convention, the ¹L_a state of the ZnP-f-anthracene corresponds to the ²A₁ state, the ¹L_a and ¹L_b states of FBP-(f-anthracene)₂ correspond to ¹B_{3u} and ¹B_{2u} states, respectively, whereas the ¹L_a state of FBP-f-coronene corresponds to the ¹B₂ state. However, it should be noted that other codes can employ different symmetry conventions, and therefore, the classification of excited states based on specifying leading excitations provides an unambiguous method of their characterization.

Before we start the discussion of the EOMCC results for the anthracene molecule, it is worth mentioning that the VEEs cannot be measured experimentally and the results of theoretical calculations can only be interpreted in terms of approximate positions of the maxima in the experimental UV absorption spectrum (for the pertinent discussion, see ref 56). For example, it was shown that even for small molecules (benzene and furan) the uncertainties can be on the order of 0.1–0.2 eV.^{57–59} Similar conclusions have been drawn for the naphthalene and anthracene molecules, where the 0–0 transition energies were estimated using the CIS method and compared to the accurate gas-phase experiments (see, for example, ref 61), showing that the CIS VEEs are 0.2–0.6 eV higher in energy than the maximum intensity peaks.⁶⁰ Other factors contributing to experiment–theory discrepancies can be attributed to the basis set quality and level of theory used to describe correlation effects. In order to make adequate comparisons, in our studies for anthracene we will use the solvent-corrected experimental VEEs of ref 62.

In previous studies various levels of theory have been applied to these systems, from TDDFT methods to the coupled cluster CC2 formalism²⁵ (see refs 62–64 and references therein). In Table 1 we show the VEEs for anthracene obtained with the AVTZ, cc-pVDZ, and POL1 basis sets. For all basis sets employed, one can observe the significant effects of the CR-EOMCCSD(T) corrections, which lower the EOMCCSD ¹L_a and ¹L_b VEEs by 0.24–0.31 eV. The best predictions of the VEEs corresponding to these states are obtained with the POL1 basis set. In both cases, the CR-EOMCCSD(T) errors are reduced to within 0.1 eV. One should also notice that all EOMCC calculations shown in Table 1 reverse the ordering of the ¹L_a and ¹L_b states. Instead of 0.04 eV above, the ¹L_b state is predicted to be 0.1 eV below the ¹L_a state. This is somewhat puzzling, since the CC2 calculations of ref 62 predict ordering consistent with the experiment, although the ¹L_a and ¹L_b separation of 0.2 eV obtained with the CC2 method is a bit exaggerated.⁶² Similar reverse ordering has been reported in the context of

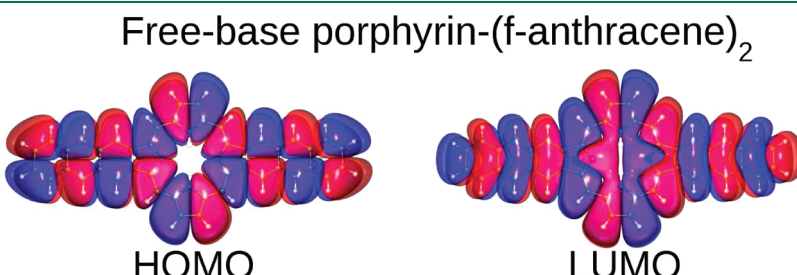


Figure 3. Graphical representation of the RHF HOMO and LUMO orbitals for the FBP-(f-anthracene)₂ system obtained with the cc-pVDZ basis set.

multireference Møller–Plesset (MRPT) theory^{66,67} calculations for low-lying excited states of anthracene (see ref 65). In the case of the MRPT approach, the 0.17 eV separation between $^1\text{L}_\text{b}$ and $^1\text{L}_\text{a}$ states is slightly larger than 0.1 eV obtained with the CR-EOMCCSD(T) method for the POL1 basis set. The discrepancies between the CR-EOMCCSD(T) and experimental vertical energies of ref 62 can be attributed to many factors including (1) basis set quality [For the $^1\text{L}_\text{a}$ state one can observe a strong effect due to the basis set quality. The difference between AVTZ and POL1 CREOMCCSD(T) VEEs for this state is as big as 0.53 eV. This difference, however, is much smaller for the $^1\text{L}_\text{b}$ state (0.17 eV) predicted to be the lowest singlet excited state by all presented EOMCC calculations.], (2) insufficient treatment of correlation effects, and (3) uncertainties of the TDDFT-based procedure of defining the experimental VEEs described in ref 62.

For the coronene molecule (Table 2), we used AVTZ, cc-pVDZ, POL1, and cc-pVTZ basis sets. The experimental value is available only for the $^1\text{L}_\text{a}$ state.⁶⁸ As can be seen from Table 2, the best estimate for the experimental VEE of the $^1\text{L}_\text{a}$ state is obtained with the CR-EOMCCSD(T) method in

cc-pVTZ basis set, where the error is reduced to 0.05 eV. The analogous error for the POL1 basis set amounts to 0.09 eV. It should be stressed that for the $^1\text{L}_\text{a}$ state a strong dependency on the basis set is observed. For example, the CR-EOMCCSD(T) predictions for the AVTZ and cc-pVTZ basis sets differ by 0.48 eV. However, for the first singlet excited state, the AVTZ and cc-pVTZ CR-EOMCCSD(T) difference is much smaller, 0.14 eV. The same is true for the cc-pVDZ basis set, although for this basis set these differences are reduced to 0.15 eV ($^1\text{L}_\text{a}$ state) and 0.08 eV ($^1\text{L}_\text{b}$ state), respectively. A similar trend can be observed for the lowest states predicted by the EOMCC methods for the anthracene molecule.

The spectral properties of anthracene fused porphyrins have recently been studied experimentally. In ref 7 it was demonstrated that the fusion to the anthracene can significantly change the electronic structure of the porphyrin, shifting the absorption maximum to the near-infrared region. Our ZnP-f-anthracene model can be used to study this effect. The ZnP-f-anthracene molecule can be considered as a model for the β,meso,β triply fused porphyrin (system 1c using the nomenclature of ref 7), which shows an absorption maximum at 725 nm (1.71 eV). Our particular goal is to establish the quality of the EOMCC methods in describing this absorption shift. In Table 3 we show the results of the EOMCCSD and CR-EOMCCSD(T) calculations with the AVTZ and cc-pVDZ basis sets. The results obtained with both basis sets show that the lowest excited state is dominated by HOMO→LUMO excitation; i.e., the lowest state can be categorized as the $^1\text{L}_\text{a}$ state. The absolute values of dominant R_K amplitudes in the cc-pVDZ basis set are as follows: $|R_{\text{L}\alpha}^{\text{H}\alpha}| = |R_{\text{L}\beta}^{\text{H}\beta}| \approx 0.57$, $|R_{\text{L}+1\alpha}^{\text{H}-1\alpha}| = |R_{\text{L}+1\beta}^{\text{H}-1\beta}| \approx 0.30$. Similar amplitude values were obtained for the AVTZ basis set. The Hartree–Fock (HF) HOMO and LUMO orbitals in the cc-pVDZ basis set are plotted in Figure 2. Moreover, both basis sets give virtually identical EOMCCSD results (2.03 eV), which are 0.32 eV above the experimental 1.71 eV value. By adding CR-EOMCCSD(T) corrections we significantly reduce the EOMCCSD errors to 0.08 and 0.06 eV for AVTZ and cc-pVDZ basis sets, respectively. The 1.77 eV CR-EOMCCSD(T) VEE for the $^1\text{L}_\text{a}$ state is in good agreement with the experimental 1.71 eV value. The CR-EOMCCSD(T)/cc-pVDZ 1.77 eV value should be compared with the VEEs 2.25, 2.25, and 3.76 eV of lowest-lying singlet excited states obtained with the CR-EOMCCSD(T) method for the zinc–porphyrin (ZnP) system.⁵⁴ It should also be stressed that for the ZnP-f-anthracene model the discrepancy between CR-EOMCCSD(T) VEEs obtained with the AVTZ and cc-pVDZ basis sets are smaller than in the case of anthracene and coronene.

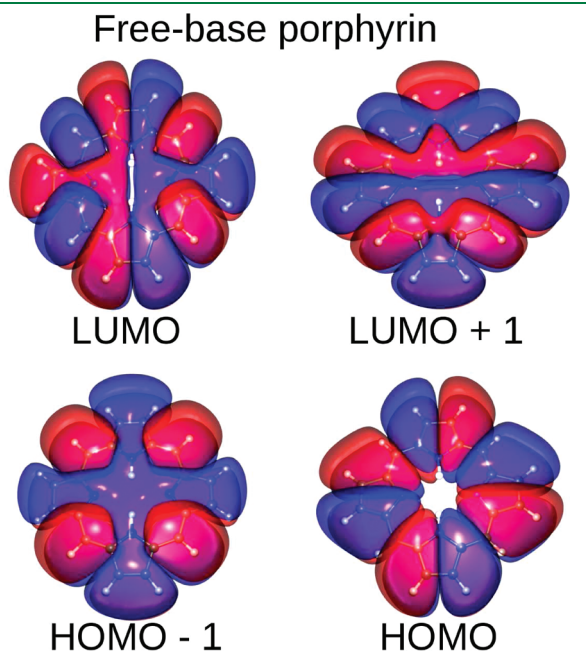


Figure 4. Graphical representation of the RHF HOMO–1, HOMO, LUMO, and LUMO+1 orbitals for the FBP molecule obtained with the cc-pVDZ basis set.

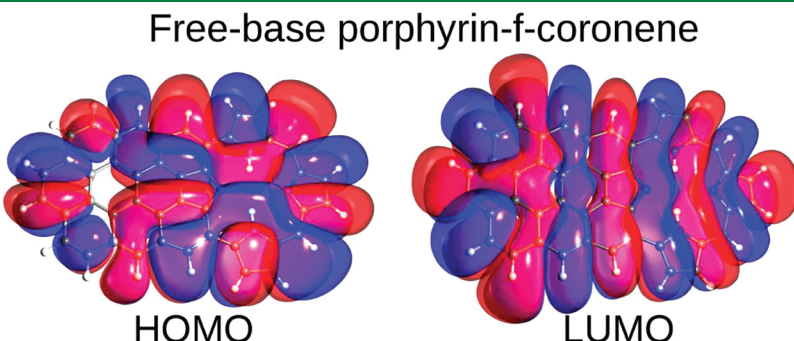


Figure 5. Graphical representation of the RHF HOMO and LUMO orbitals for the FBP-f-coronene system obtained with the AVTZ basis set.

The results discussed above indicate that for larger systems the lowest excited state can be satisfactorily described by the AVTZ or cc-pVDZ basis sets. Using these basis sets we will evaluate the effect of functionalizing free base porphyrin with one- and two-dimensional structures. These problems will be studied with our FBP-(f-anthracene)₂ and FBP-f-coronene models. The results of our calculations are shown in Table 4. For the FBP-(f-anthracene)₂ system we employed the cc-pVDZ basis set, which for ¹L_a and ¹L_b states gives EOMCCSD VEEs equal to 1.99 and 2.57 eV, respectively. As in the ZnP-f-anthracene model, the inclusion of the CR-EOMCCSD(T) corrections lowers the EOMCCSD VEEs to 1.78 and 2.37 eV, respectively. This should be compared with the CR-EOMCCSD(T) energies of 1.86 and 2.32 eV corresponding to the ¹B_{3u} and ¹B_{2u} states of FBP.³⁵ In order to understand the nature of the ¹L_a and ¹L_b states, we plotted the cc-pVDZ HF HOMO and LUMO orbitals of FBP-(f-anthracene)₂ and HOMO-1, HOMO, LUMO, LUMO+1 orbitals of FBP; see Figures 3 and 4, respectively. There are two notable features of the FBP-(f-anthracene)₂'s HOMO and LUMO orbitals. First, both orbitals are delocalized over the whole system. Second, the parts of the FBP-(f-anthracene)₂ HOMO and LUMO orbitals localized on FBP bear great resemblance to the FBP's HOMO and LUMO orbitals. Given that the largest contribution to this state comes from the HOMO-LUMO excitation ($|R_{L\alpha}^{H\alpha}| = |R_{L\beta}^{H\beta}| \approx 0.54$ for the cc-pVDZ basis set) and the second largest contribution to the ¹L_a state corresponds to the HOMO-1→LUMO+1 excitation ($|R_{L+1\alpha}^{H-1\alpha}| = |R_{L+1\beta}^{H-1\beta}| \approx 0.36$ for the cc-pVDZ basis), the ¹L_a should be attributed to the ¹B_{2u} state of FBP ($|R_{L\alpha}^{H\alpha}| = |R_{L\beta}^{H\beta}| \approx 0.48$ and $|R_{L+1\alpha}^{H-1\alpha}| = |R_{L+1\beta}^{H-1\beta}| \approx 0.45$ in the cc-pVDZ basis set), which corresponds to 0.54 eV red-shift using CR-EOMCCSD(T) results. It is also interesting to notice that the CR-EOMCCSD(T) method yields almost identical estimates for the ¹L_a states of the FBP-(f-anthracene)₂ and ZnP-f-anthracene systems. The ¹L_b state of FBP-(f-anthracene)₂ is dominated by the HOMO-1→LUMO and HOMO→LUMO+1 excitations ($|R_{L+1\alpha}^{H\alpha}| = |R_{L+1\beta}^{H\beta}| \approx 0.52$, $|R_{L\alpha}^{H-1\alpha}| = |R_{L\beta}^{H-1\beta}| \approx 0.40$ in the cc-pVDZ basis set) and bears a resemblance to the ¹B_{3u} state of FBP ($|R_{L\alpha}^{H-1\alpha}| = |R_{L\beta}^{H-1\beta}| \approx 0.48$, $|R_{L+1\alpha}^{H\alpha}| = |R_{L+1\beta}^{H\beta}| \approx 0.43$ in the cc-pVDZ basis set).

Due to its size, the calculations for the FBP-f-coronene model were performed only for the ¹L_a state in the AVTZ basis set. From Table 4 it is evident that the effect of functionalization of FBP with coronene has much stronger effects than when anthracene is used. The EOMCCSD VEE corresponding to the ¹L_a state is equal 1.63 eV, while the CR-EOMCCSD(T) yields 1.36 eV, which is more than 0.4 eV below the ¹L_a VEEs for the FBP-(f-anthracene)₂ and ZnP-f-anthracene systems. The HOMO and LUMO orbitals are shown in Figure 5. The ¹L_a is almost entirely dominated by the HOMO→LUMO excitation ($|R_{L\alpha}^{H\alpha}| = |R_{L\beta}^{H\beta}| \approx 0.64$ in the AVTZ basis set). It is interesting to note that the HOMO orbital is to a large extent localized on the FBP component and on the buffer region between FBP and coronene. The opposite tendency can be observed for the LUMO orbital, which is mostly localized on the coronene component.

■ PARALLEL PERFORMANCE

In all CC/EOMCC calculations reported in this paper, in-core algorithms were used. All cluster/excitation amplitudes, electron integrals, and recursive intermediates were stored in global arrays (GA).⁶⁹ GA forms an abstraction layer that alleviates the task of the developer by isolating most of the complexities involved in parallelizing

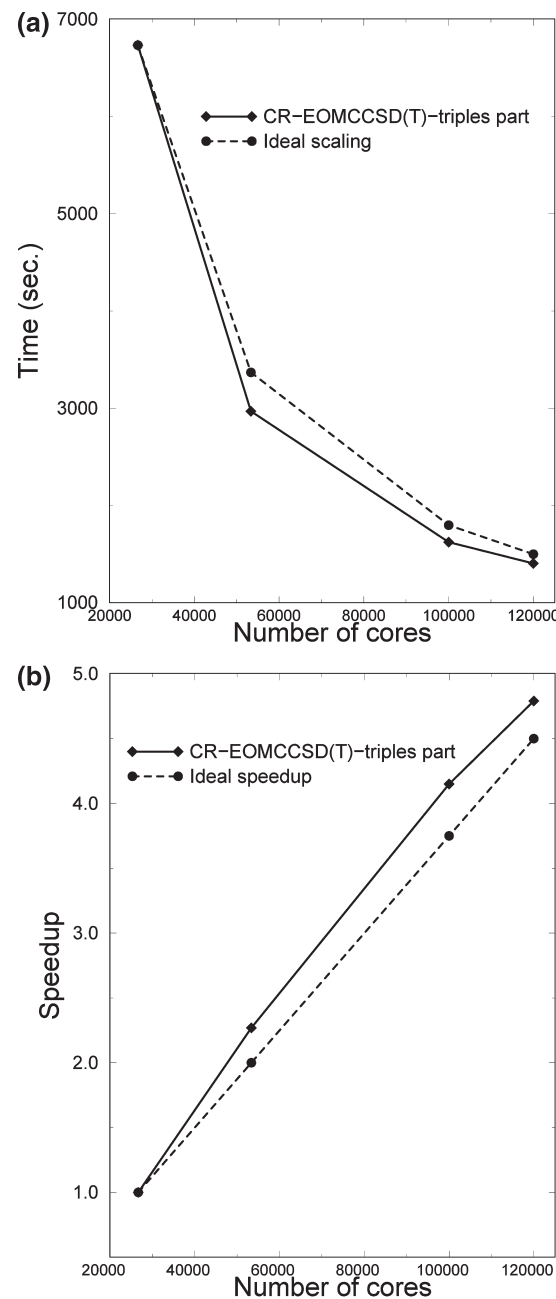


Figure 6. Scalability of the triples part of the CR-EOMCCSD(T) approach for the FBP-f-coronene system in the AVTZ basis set: (a) the time to solution as a function of the number of cores and (b) the corresponding speedups. Timings were determined from calculations on the Jaguar Cray XT5 computer system at NCCS (ORNL).

software that make use of dense matrices. It relies on several components: a message passing library, the ARMCI one-sided communication library, and a memory allocator (MA library). Most of the NWChem modules (including the ones used for this work) make very little use of MPI, since the majority of the communication is managed by the ARMCI one-sided communication library.

In some cases we also employed the CCSD/EOMCCSD implementations utilizing a new task scheduling approach based on the global task pool. Typical timings characterizing our calculations can be summarized as follows.

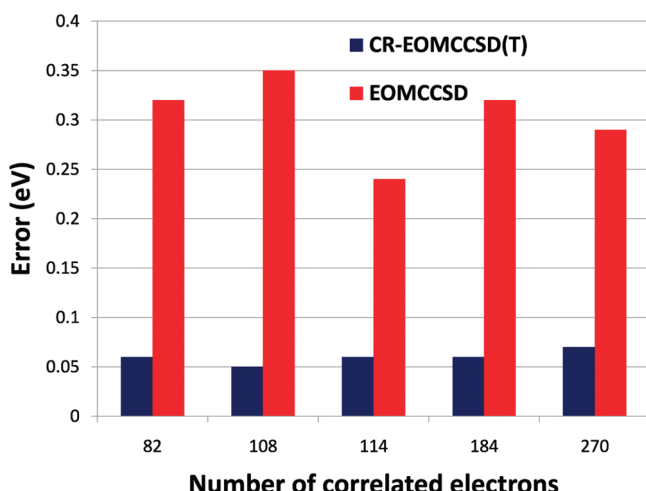


Figure 7. The EOMCCSD and CR-EOMCCSD(T) errors with respect to the experimentally available data for the green fluorescent protein chromophore, coronene, FBP, and oligoporphyrin dimer molecules (see the text for details).

- The coronene molecule in the cc-pVTZ basis set (888 basis set functions, 1020 cores, Chinook HP at EMSL): CCSD iteration, 5.5 min; EOMCCSD iteration, 5.9 min; recursive intermediates for the triples part of the CR-EOMCCSD(T) approach, 28.5 min; triples part of the CR-EOMCCSD(T) method, 2.7 h.
- The FBP-(f-anthracene)₂ system in the cc-pVDZ basis set (802 basis set functions, 1020 cores, Chinook HP at EMSL): CCSD iteration, 21.5 min; EOMCCSD iteration, 21.5 min; recursive intermediates for the triples part of the CR-EOMCCSD(T) approach, 1.48 h; triples part of the CR-EOMCCSD(T) method, 9.6 h.
- The FBP-f-coronene system in the AVTZ basis set (780 basis set functions, 4096 cores, Jaguar Cray XT5 at ORNL): CCSD iteration, 21.3 min; EOMCCSD iteration, 22.8 min; CR-EOMCCSD(T) recursive intermediates, 2.1 h. All these calculations were performed using eight cores per 12 core node. It means that effectively 6144 cores have been used. The scalability of the triples part of the CR-EOMCCSD(T), which is characterized by the N^7 complexity, is shown in Figures 6a,b. In our test calculations this part of code was characterized by a very good parallel performance across 120 000 cores. For example, the 6733 s required by the triples part on 26 672 cores is reduced to 2968, 1623, and 1404 s when 53 326, 100 016, and 120 000 cores are used, respectively. Again, in these tests eight cores per 12 core node have been used, which means that 180 000 cores have been allocated in the largest calculation. Since future parallel architectures may be characterized by smaller memory per core, we performed one calculation for 100 008 cores using all (12) cores per node. The obtained timing of 1787 s is only slightly worse than the 1623 s obtained with 100 016 cores when eight cores per node are used. For eight cores per node calculations we used 600 and 600 MB partitioning for local and global memory, respectively, while in the 12 core per node run we used 600 and 300 MB allocations for the two types of memory. In order to properly address the local memory bottleneck, we have developed the new version of the CR-EOMCCSD(T) approach where all six-dimensional

tensors can be dynamically “sliced” across first two dimensions in order to match available local memory.

CONCLUSIONS

The functionalization of the porphyrins with two-dimensional structures (in the current studies coronene was used) has stronger effects than the functionalization with one-dimensional structures (anthracene). While for the two types of anthracene functionalization considered here the resulting VEEs for lowest excited states of functionalized porphyrins have similar values, the functionalization of the FBP with coronene significantly shifts the VEE of the lowest excited state into the infrared region. We also demonstrated that the functionalization of the porphyrins with the anthracene or coronene significantly alters the electronic structure of the low-lying excited states. Instead of the multiconfigurational character of the lowest excited states of the FBP and ZnP systems, we showed that the lowest states of the ZnP-f-anthracene, FBP-(f-anthracene)₂, and FBP-f-coronene systems are dominated by the HOMO–LUMO excitations. For the ZnP-f-anthracene, the CR-EOMCCSD(T) approach, in the modest AVTZ and cc-pVDZ basis sets, is capable of reproducing the experimental excitation energies to within 0.1 eV. The remaining errors can be attributed to basis set effects, missing correlation effects, and simplified representation of the true molecular system used in the experiment. At the same time, the results obtained for anthracene and coronene suggest that for the VEEs corresponding to higher excited states, basis set effects play an important role. We have also demonstrated that the N^7 part of the CR-EOMCCSD(T) calculations can take advantage of a large number of cores and the scalability across 120 000 cores can be achieved.

Our last conclusion concerns the effect of higher-order correlation effects in describing the VEEs for large systems. It was demonstrated in the previous studies that while for singly excited states the EOMCCSD approach provides a good description of corresponding VEEs, for the proper description of doubly excited states including the effect of triply excited configurations is indispensable for the qualitative accuracy of the EOMCC calculations.³³ Since these conclusions were inferred from calculations for small molecular systems, it is important to answer the same question about the role of particular correlation effects for large systems. The results of this paper in conjunction with previous studies³⁵ will help us to understand these problems at least for singly excited states. Figure 7 contains the deviations of the EOMCCSD and CR-EOMCCSD(T) results from the available experimental values for several systems of different size: Green Fluorescent Protein Chromophore (82 correlated electrons, POL1 basis set), coronene (108 correlated electrons, cc-pVTZ basis set), FBP (114 correlated electrons, POL1 basis set), ZnP-f-anthracene (184 correlated electrons, cc-pVDZ basis set), and oligoporphyrin dimer P₂TA^{10,70} (270 correlated electrons, cc-pVDZ basis set). Although various quality of basis sets have been used, the general trend can be clearly seen from the Figure 7. One can notice that noniterative CR-EOMCCSD(T) corrections significantly reduce the absolute values of the 0.24–0.35 eV EOMCCSD errors to 0.05–0.07 eV (see Figure 7), which clearly demonstrate the increasingly more important role played by triple excitations for singly excited states of larger molecular systems. Similar studies for doubly excited states of large systems are facing problems with locating doubly excited states, which are shifted upward in the energy spectrum by the EOMCCSD method. For this purpose, in

the coming studies we will use the sequence of the EOMCCD, EOMCCSD, and CR-EOMCCSD(T) calculations. The role of the EOMCCD approximation will be to identify the lowest lying doubly excited states, which can be used as a starting vectors for the EOMCCSD approach.

Although the comparison of the EOMCC results with the TDDFT ones is beyond the scope of this paper, it is worth mentioning that while for the anthracene, coronene, ZnP-f-anthracene, and FBP-(f-anthracene)₂ the CR-EOMCCSD(T) and CAM-B3LYP¹² results are in a good agreement, for the FBP-f-coronene one can observe significant discrepancy between the CR-EOMCCSD(T) and CAM-B3LYP excitation energies corresponding to the lowest singlet excited state⁷¹ obtained for the same AVTZ basis set.

■ AUTHOR INFORMATION

Corresponding Author

*E-mail: karol.kowalski@pnl.gov (K.K.), aprae@ornl.gov (E.A.).

■ ACKNOWLEDGMENT

The work related to the development of the scalable EOMCCSD and CR-EOMCCSD(T) approaches (K.K.) and development of new parallel tools (S.K.) was supported by the Extreme Scale Computing Initiative, a Laboratory Directed Research and Development Program at Pacific Northwest National Laboratory. Most of the calculations have been performed using EMSL, a national scientific user facility sponsored by the Department of Energy's Office of Biological and Environmental Research and located at Pacific Northwest National Laboratory. The Pacific Northwest National Laboratory is operated for the U.S. Department of Energy by the Battelle Memorial Institute under Contract DE-AC06-76RLO-1830. The scalability tests of the CR-EOMCCSD(T) implementation of NWChem have been performed on the Jaguar Cray-XT5 computer system of the National Center for Computational Sciences at Oak Ridge National Laboratory, which is supported by the Office of Science of the U.S. Department of Energy under Contract No. DE-AC05-00OR22725.

■ REFERENCES

- (1) Tsuda, A.; Furuta, H.; Osuka, A. *Angew. Chem., Int. Ed.* **2000**, *39*, 2549–2552.
- (2) Tsuda, A.; Furuta, H.; Osuka, A. *J. Am. Chem. Soc.* **2001**, *123*, 10304–10321.
- (3) Tsuda, A.; Osuka, A. *Science* **2001**, *293*, 79–82.
- (4) Anthony, J. E. *Chem. Rev.* **2006**, *106*, 5028–5048.
- (5) Wu, J.; Pisula, W.; Müllen, K. *Chem. Rev.* **2007**, *107*, 718–747.
- (6) Müllen, K.; Rabe, J. P. *Acc. Chem. Res.* **2008**, *41*, 511–520.
- (7) Davis, N. K. S.; Pawlicki, M.; Anderson, H. L. *Org. Lett.* **2008**, *10*, 3945–3947.
- (8) Brédas, L. L.; Norton, J. E.; Cornil, J.; Coropceanu, V. *Acc. Chem. Res.* **2009**, *42*, 1691–1699.
- (9) Imahorii, H.; Umeyama, T.; Ito, S. *Acc. Chem. Res.* **2009**, *42*, 1809–1818.
- (10) Reimers, J. R.; Hall, L. E.; Crossley, M. J.; Hush, N. S. *J. Phys. Chem. A* **1999**, *103*, 4385–4397.
- (11) Iikura, H.; Tsuneda, T.; Yanai, T.; Hirao, K. *J. Chem. Phys.* **2001**, *115*, 35403544.
- (12) Yanai, T.; Tew, D. P.; Handy, N. C. *Chem. Phys. Lett.* **2004**, *393*, 51–57.
- (13) Jensen, L.; Govind, N. *J. Phys. Chem. A* **2009**, *113*, 9761–9765.
- (14) Peach, M. J. G.; Helgaker, T.; Salek, P.; Keal, T. W.; Lutnaes, O. B.; Tozer, D. J.; Handy, N. C. *Phys. Chem. Chem. Phys.* **2006**, *8*, 558–562.
- (15) Tokura, S.; Yagi, K.; Tsuneda, T.; Hirao, K. *Chem. Phys. Lett.* **2007**, *436*, 30–35.
- (16) Glaesemann, K. R.; Govind, N.; Krishnamoorthy, S.; Kowalski, K. *J. Phys. Chem. A* **2010**, *114*, 8764–8771.
- (17) Bartlett, R. J.; Musiał, M. *Rev. Mod. Phys.* **2007**, *79*, 291–352.
- (18) Geersten, J.; Rittby, M.; Bartlett, R. J. *Chem. Phys. Lett.* **1989**, *164*, 57–62.
- (19) Comeau, D. C.; Bartlett, R. J. *Chem. Phys. Lett.* **1993**, *207*, 414–423.
- (20) Stanton, J. F.; Bartlett, R. J. *J. Chem. Phys.* **1993**, *98*, 7029–7039.
- (21) Monkhorst, H. J. *Int. J. Quantum Chem.* **1977**, *S11*, 421–432.
- (22) Dalgaard, E.; Monkhorst, H. J. *Phys. Rev. A* **1983**, *28*, 1217–1222.
- (23) Koch, H.; Jørgensen, P. *J. Chem. Phys.* **1990**, *93*, 3333–3344.
- (24) Nakatsuji, H.; Hirao, H. *J. Chem. Phys.* **1978**, *69*, 4535–4547.
- (25) Christiansen, O.; Koch, H.; Jørgensen, P. *Chem. Phys. Lett.* **1995**, *243*, 409–418.
- (26) Christiansen, O.; Koch, H.; Jørgensen, P. *J. Chem. Phys.* **1995**, *103*, 7429–7441.
- (27) Christiansen, O.; Koch, H.; Jørgensen, P.; Olsen, J. *Chem. Phys. Lett.* **1996**, *256*, 185–194.
- (28) Nooijen, M. *J. Chem. Phys.* **1996**, *104*, 2638–2651.
- (29) Krylov, A. I. *Chem. Phys. Lett.* **2001**, *338*, 375–384.
- (30) Musiał, M.; Bartlett, R. J. *J. Chem. Phys.* **2011**, *134*, 034106.
- (31) Kowalski, K.; Piecuch, P. *J. Chem. Phys.* **2001**, *115*, 643–651.
- (32) Hirata, S. *J. Chem. Phys.* **2004**, *121*, 51–59.
- (33) Kowalski, K.; Piecuch, P. *J. Chem. Phys.* **2004**, *120*, 1715–1738.
- (34) Kowalski, K.; Piecuch, P. *J. Chem. Phys.* **2001**, *115*, 2966–2978.
- (35) Kowalski, K.; Krishnamoorthy, S.; Villa, O.; Hammond, J. R.; Govind, N. *J. Chem. Phys.* **2010**, *132*, 154103.
- (36) Watts, J. D.; Bartlett, R. J. *Chem. Phys. Lett.* **1995**, *233*, 81–87.
- (37) Watts, J. D.; Bartlett, R. J. *Chem. Phys. Lett.* **1996**, *258*, 581–588.
- (38) Christiansen, O.; Koch, H.; Jørgensen, P. *J. Chem. Phys.* **1996**, *105*, 1451–1459.
- (39) Hirata, S.; Nooijen, M.; Grabowski, I.; Bartlett, R. J. *J. Chem. Phys.* **2001**, *114*, 3919–3928.
- (40) Shiozaki, T.; Hirao, K.; Hirata, S. *J. Chem. Phys.* **2007**, *126*, 244106.
- (41) Manohar, P. U.; Krylov, A. I. *J. Chem. Phys.* **2008**, *129*, 194105.
- (42) Włoch, M.; Lodriguito, M. D.; Piecuch, P.; Gour, J. R. *Mol. Phys.* **2006**, *104*, 2149–2172.
- (43) Piecuch, P.; Gour, J. R.; Włoch, M. *Int. J. Quantum Chem.* **2009**, *109*, 3268–3304.
- (44) Kowalski, K. *J. Chem. Phys.* **2009**, *130*, 194110.
- (45) Raghavachari, K.; Trucks, G. W.; Pople, J. A.; Head-Gordon, M. *Chem. Phys. Lett.* **1989**, *157*, 479–483.
- (46) Valiev, M.; Bylska, E. J.; Govind, N.; Kowalski, K.; Straatsma, T. P.; van Dam, H. J. J.; Wang, D.; Nieplocha, J.; Aprà, E.; Windus, T. L.; de Jong, W. A. *Comput. Phys. Commun.* **2010**, *181*, 1477–1489.
- (47) Hirata, S. *J. Phys. Chem. A* **2003**, *107*, 9887–9897.
- (48) Stephens, P. J.; Devlin, F. J.; Chabalowski, C. F.; Frisch, M. J. *J. Phys. Chem.* **1994**, *98*, 11623–11627.
- (49) Dunning, T. H. *J. Chem. Phys.* **1989**, *90*, 1007–1023.
- (50) Balabanov, N. B.; Peterson, K. A. *J. Chem. Phys.* **2005**, *123*, 064107.
- (51) Hammond, J. R.; de Jong, W. A.; Kowalski, K. *J. Chem. Phys.* **2007**, *127*, 144105.
- (52) Sekino, H.; Kobayashi, H. *J. Chem. Phys.* **1981**, *75*, 3477–3484.
- (53) Sadlej, A. J. *Collect. Czech. Chem. Commun.* **1988**, *53*, 1995–2016.
- (54) Schafer, A.; Horn, H.; Ahlrichs, R. *J. Chem. Phys.* **1992**, *97*, 2571–2577.
- (55) Fan, P. D.; Valiev, M.; Kowalski, K. *Chem. Phys. Lett.* **2008**, *458*, 205–209.
- (56) Platt, J. R. *J. Chem. Phys.* **1949**, *17*, 484–495.
- (57) Bak, K. L.; Koch, H.; Oddershede, J.; Christiansen, J.; Sauer, S. P. A. *J. Chem. Phys.* **2000**, *112*, 4173–4185.
- (58) Christiansen, O.; Jørgensen, P. *J. Am. Chem. Soc.* **1998**, *120*, 3423–3430.

- (58) Christiansen, O.; Koch, H.; Jørgensen, P.; Helgaker, T.; de Merás, A. S. *J. Chem. Phys.* **1996**, *105*, 6921–6939.
- (59) Christiansen, O.; Stanton, J. F.; Gauss, J. *J. Chem. Phys.* **1998**, *108*, 3987–4001.
- (60) Jas, G. S.; Kuczera, K. *Chem. Phys.* **1997**, *214*, 229–241.
- (61) Lambert, W. R.; Felker, P. M.; Syage, J. A.; Zewail, A. H. *J. Chem. Phys.* **1984**, *81*, 2195–2207.
- (62) Grimme, S.; Parac, M. *ChemPhysChem* **2003**, *4*, 292–295.
- (63) Parac, M.; Grimme, S. *Chem. Phys.* **2003**, *292*, 11–21.
- (64) Wong, B. M.; Hsieh, T. H. *J. Chem. Theory Comput.* **2010**, *6*, 3704–3712.
- (65) Kawashima, Y.; Hashimoto, T.; Nakano, H.; Hirao, K. *Theor. Chem. Acc.* **1998**, *102*, 49–64.
- (66) Hirao, K. *Chem. Phys. Lett.* **1992**, *190*, 374–380.
- (67) Hirao, K. *Chem. Phys. Lett.* **1992**, *196*, 397–403.
- (68) Birks, J. B. *Photophysics of Aromatic Molecules*; Wiley: New York, 1970.
- (69) Nieplocha, J.; Harrison, R. J.; Littlefield, R. J. Global Arrays: A Portable Shared-Memory Programming Model for Distributed Memory Computers. In *Proceedings of Supercomputing 94*; IEEE CS Press: Washington, DC, 1994; 340349. Nieplocha, J.; Harrison, R. J.; Littlefield, R. J. *J. Supercomput.* **1996**, *10*, 169–189.
- (70) Sendt, K.; Johnston, L. A.; Hough, W. A.; Crossley, M. J.; Hush, N. S.; Reimers, J. R. *J. Am. Chem. Soc.* **2002**, *124*, 9299–9309.
- (71) Aprà E.; Lopata, K.; Govind, N.; Kowalski, K. Manuscript in preparation.